

# Standard Thermodynamic Properties of H<sub>3</sub>PO<sub>4</sub>(aq) over a Wide Range of Temperatures and Pressures

Karine Ballerat-Busserolles,<sup>†</sup> Josef Sedlbauer,<sup>‡</sup> and Vladimir Majer<sup>\*,†</sup>

Laboratoire de Thermodynamique des Solutions et des Polymères, Université Blaise Pascal Clermont-Ferrand/CNRS, 63177 Aubière, France, and the Department of Chemistry, Technical University Liberec, 461 17 Liberec, Czech Republic

Received: July 21, 2006; In Final Form: September 29, 2006

The densities and heat capacities of solutions of phosphoric acid, 0.05 to 1 mol kg<sup>-1</sup>, were measured using flow vibrating tube densitometry and differential Picker-type calorimetry at temperatures up to 623 K and at pressures up to 28 MPa. The standard molar volumes and heat capacities of molecular H<sub>3</sub>PO<sub>4</sub>(aq) were obtained, via the apparent molar properties corrected for partial dissociation, by extrapolation to infinite dilution. The data on standard derivative properties were correlated simultaneously with the dissociation constants of phosphoric acid from the literature using the theoretically founded SOCW model. This made it possible to describe the standard thermodynamic properties, particularly the standard chemical potential, of both molecular and ionized phosphoric acid at temperatures up to at least 623 K and at pressures up to 200 MPa. This representation allows one to easily calculate the first-degree dissociation constant of H<sub>3</sub>PO<sub>4</sub>(aq). The performance of the SOCW model was compared with the other approaches for calculating the high-temperature dissociation constant of the phosphoric acid. Using the standard derivative properties, sensitively reflecting the interactions between the solute and the solvent, the high-temperature behavior of H<sub>3</sub>PO<sub>4</sub>(aq) is compared with that of other weak acids.

## Introduction

Thermodynamic properties of aqueous phosphoric acid at superambient conditions, particularly its dissociation constant, are of both technological and geochemical interest. Concentrated solutions of H<sub>3</sub>PO<sub>4</sub>(aq) are used as electrolytes in fuel cells operating typically at temperatures from 425 to 550 K. Phosphate ions, as water softeners and buffering agents, can be present in power cycles where temperatures may reach beyond the critical point of water. Because phosphate salts are a part of numerous minerals and common fertilizers, phosphoric acid and its anions are also encountered in underground waters and hydrothermal systems.

Phosphoric acid is not a particularly strong acid; its first-degree dissociation constant is on the order of 10<sup>-3</sup> at ambient conditions, with the other two higher-degree dissociation constants being much lower (orders of 10<sup>-8</sup> and 10<sup>-12</sup>). While the presence of divalent and trivalent ions can be neglected in the H<sub>3</sub>PO<sub>4</sub>(aq) solutions, the first-order dissociation is considerable at room temperatures, higher than for acetic acid, for example. For nominal concentrations between 0.1 and 1 mol kg<sup>-1</sup>, the percentage of dissociated H<sub>3</sub>PO<sub>4</sub>(aq) is between 30 and 10%, but the portion of ionic species decreases with increasing temperature due to the decreasing dielectric constant of water, and the dissociation is not considered as important at temperatures above 573 K.

There are not much thermodynamic data available on solutions of phosphoric acids at superambient conditions, and the possibilities of calculating the speciation of H<sub>3</sub>PO<sub>4</sub>(aq) as a function of temperature and pressure are therefore limited. The

common tool available for such a calculation is the software SUPCRT92,<sup>1</sup> largely used by geochemists for prediction of thermodynamic reaction constants at hydrothermal conditions. It is based on a revised version of a semiempirical model of Helgeson, Kirkham, and Flowers (HKF);<sup>2</sup> its parameters were adjusted for the molecular acid and its univalent ion using a limited number of high-temperature first-degree dissociation constants of H<sub>3</sub>PO<sub>4</sub>(aq) and the reference thermodynamic data for molecular and ionized acid at 298 K and 0.1 MPa.<sup>3,4</sup> It was noted in the literature<sup>5</sup> that, while the HKF model is able to properly describe the standard thermodynamic properties of ions at high temperatures, it is not well adapted for representation of nonelectrolyte species. The model is based on the use of the Born equation for expressing hydration of an ion and has therefore no theoretical justification for predictions with nonelectrolyte solutes.

Our main objective was to improve the possibilities of calculating the standard thermodynamic properties for both molecular and ionized phosphoric acid in aqueous solution over a wide range of temperatures and pressures using new experimental data and a better theoretically founded model. This information is useful for calculation of the thermodynamic reaction constants, particularly the first-degree ionization of H<sub>3</sub>PO<sub>4</sub>(aq)



$$\ln K_{\text{dis}} = -\Delta_{\text{dis}} G^\circ / (RT) = -(G_s^\circ(\text{H}_2\text{PO}_4^-) - G_s^\circ(\text{H}_3\text{PO}_4)) / (RT) \quad (2)$$

where  $G_s^\circ(\text{H}_2\text{PO}_4^-)$  and  $G_s^\circ(\text{H}_3\text{PO}_4)$  are the standard chemical potentials of the ionized and molecular acid, respectively;

\* Corresponding author. E-mail: Vladimir.Majer@univ-bpclermont.fr.

<sup>†</sup> Université Blaise Pascal Clermont-Ferrand.

<sup>‡</sup> Technical University Liberec.

according to the generally accepted convention, it is considered that  $G_s^{\circ}(\text{H}^+) = 0$ .

In the experimental part of this study, we have carried out precise densitometric and heat capacity measurements with dilute solutions of phosphoric acid at temperatures up to 573 and 623 K, respectively, and at pressures close to the saturation line of water and at 28 MPa. The experimental values were used to obtain, by extrapolation to infinite dilution, the standard molar volumes and heat capacities via the apparent molar properties  $Y_{\phi}^{\text{exp}}$

$$Y_{\phi}^{\text{exp}} = (Y - 55.5Y_w)/m \quad Y = V, C_p \quad (3)$$

where  $Y$  relates to a solution containing 1 kg of  $\text{H}_2\text{O}$  and where  $Y_w$  is a molar property of water. These experimental, apparent molar properties were corrected for the presence of ions in order to obtain the standard derivative properties for the molecular acid. The calorimetric measurements were carried out in a wider temperature range since, compared to the standard molar volume, the standard molar heat capacities change much faster with temperature and pressure and are therefore more difficult to extrapolate.

In the computational part, the newly determined standard molar volumes and heat capacities were combined with the other literature values, including the high-temperature dissociation constants, and correlated simultaneously by means of a hydration model SOCW<sup>6,7</sup> inspired by the fluctuation solution theory.<sup>8,9</sup> This semi-theoretical model has already proved to be useful, for example, in an analogous case of representing the standard thermodynamic properties of acetic acid and of the acetate ion.<sup>10</sup> The performance of the SOCW model was compared with the HKF model and with the thermodynamic integration exclusively using the standard thermodynamic data at the reference conditions of 298 K and 0.1 MPa. Finally, the high-temperature behavior of  $\text{H}_3\text{PO}_4(\text{aq})$  is compared to that of other weak acids using the standard derivative properties, sensitively reflecting the interactions between the solute and the solvent.

## Experimental Section

**Preparation of Solutions.** The solution of 85% w/w phosphoric acid in water ACS Reagent was purchased from Aldrich and directly used without further purification. The exact concentration of the mother solution of phosphoric acid was determined by titrating a solution of  $\text{H}_3\text{PO}_4$  (concentration near 1 mol  $\text{kg}^{-1}$ ) with a commercial solution of sodium hydroxide (1 N) from Acros Organics. The uncertainty in solution molalities is believed to be lower than  $\pm 0.2\%$ , considering the precision of the balance and the titration procedure used.

Solutions of interest were prepared by mass dilution of the mother solution with deionized water, which was freshly degassed under reduced pressure before use. The range of molality covered was from 0.05 to 1 mol  $\text{kg}^{-1}$ . For each experimental temperature and pressure, typically three to four different concentrations were studied. Each sample solution was generally measured at least twice in order to verify good data reproducibility. The correct function of the instruments used for measurements was controlled by the experiments with the NaCl solutions (0.05–3 mol  $\text{kg}^{-1}$ ), where the recommended data are available in the literature.<sup>11</sup>

**Volumetric Measurements.** Values of the apparent molar volumes,  $V_{\phi}^{\text{exp}}$ , were calculated from the experimental densities

using the equation

$$V_{\phi}^{\text{exp}} = \frac{M_s}{\rho_w + \Delta\rho} - \frac{\Delta\rho}{m(\rho_w + \Delta\rho)\rho_w} \quad (4)$$

where  $M_s$  is the molar mass of the solute and where  $m$  is molality of the solution;  $\rho_w$  and  $\Delta\rho$  are the density of water and the measured density difference between a solution and water, respectively.

Differences between the density of solutions and water were obtained at temperatures from 298 to 573 K and pressures up to 28 MPa using a vibrating tube densitometer described in detail by Hynek et al.<sup>12</sup> The instrument operates with a platinum–rhodium tube (1.6 mm o.d.) oscillating in a field of two permanent magnets at a resonance frequency near 133 Hz. The temperature was measured with a customized 500  $\Omega$  secondary standard from Burns Engineering with an accuracy of 0.05 K. The stability of the temperature is insured by a system of superposed, thermally regulated jackets and lids surrounding the block housing the vibrating tube. The short-term temperature stability of the densitometer block over one experiment is  $\pm 0.01$  K. The measurements were performed in a flow regime at a constant flow rate near  $8.3 \times 10^{-3} \text{ cm}^3 \text{ s}^{-1}$ . The pressure was controlled with a stability of  $\pm 0.05$  MPa using a Circle Seal back-pressure regulator at the end of the flow system and was measured by a DPI 260 Druck electronic pressure gauge with an accuracy of 0.03 MPa. A six-port valve connected with a sample loop allowed alternative introduction of water and pressurized solution samples into the flow system.

The densities were also measured with a commercial Sodev–Picker vibrating tube densitometer (type 03D<sup>13</sup>) at 298.15 K and 0.1 MPa using a lower flow rate ( $1.7 \times 10^{-3} \text{ cm}^3 \text{ s}^{-1}$ ). The temperature was maintained constant at 298.15 K within 0.005 K using a Picker thermoregulation system and was measured with an accuracy of 0.01 K. The results were consistent with those obtained on the high-temperature instrument and were treated together.

The differences between the densities of solution,  $\rho$ , and water,  $\rho_w$ , were calculated as

$$\Delta\rho = \rho - \rho_w = K(\tau^2 - \tau_w^2) \quad (5)$$

comparing the periods of oscillation of the vibrating tube containing selected solution,  $\tau$ , and pure water,  $\tau_w$ . The constancy of the two periods during an experiment are typically on the order of  $10^{-5}$  ms. The calibration constant,  $K$ , was determined at each experimental temperature and pressure by measurements with a 3 mol  $\text{kg}^{-1}$  NaCl solution up to 423 K and with pure nitrogen at higher temperatures where the data on NaCl(aq) are not available with sufficient accuracy. The density of water was calculated from the equation of Hill,<sup>14</sup> and the density of the NaCl solution was obtained from the representative correlation by Archer.<sup>11</sup> The relative error in  $K$  for the high-temperature densitometer was estimated to be 0.3% based on the reproducibility of the calibration experiments and accuracy of the densities of the fluids used in calibration. The Sodev–Picker densitometer was calibrated by comparing the vibration periods corresponding to water and vacuum in the tube, and the calibration constant was calculated with an accuracy of 0.1%.

Apparent molar volumes of phosphoric acid solutions were determined for six different temperatures and at two or three pressures between the saturation pressure of water and 28 MPa. The multiple measurements for several concentrations (0.01 to 1 mol  $\text{kg}^{-1}$ ) led to the determination of 134 new data points

for the determination of  $V_{\phi}^{\text{exp}}$ . For all conditions of  $T$  and  $p$ ,  $V_{\phi}^{\text{exp}}$  is typically slightly increasing with concentration. The concentration dependence is linear for temperatures up to 423 K but becomes concave for higher temperatures. The error in  $V_{\phi}^{\text{exp}}$  is calculated as a propagation of the uncertainty in the density difference,  $\Delta\rho$  (eq 3), that was obtained as a statistical estimate, taking into account the fluctuations in  $\tau$  and  $\tau_w$  and the systematic errors in  $K$  and the sample concentration. The experimental density differences, apparent molar volumes, and their estimated errors are available integrally in an electronic supplement (see below).

**Heat Capacity Measurements.** Values of apparent molar heat capacities,  $C_{p,\phi}^{\text{exp}}$ , were calculated from the experimental data using the following equation:

$$\begin{aligned} C_{p,\phi}^{\text{exp}} &= M_s c_p + (c_p - c_{p,w})/m \\ &= c_{p,w} \{ (M_s + 1/m) c_p / c_{p,w} - 1/m \} \end{aligned} \quad (6)$$

where  $c_p$  and  $c_{p,w}$  are the specific heat capacities of the solution and water, respectively. The specific heat capacity ratio,  $c_p/c_{p,w}$ , was determined using a high-temperature/high-pressure Picker-type differential flow calorimeter at temperatures up to 623 K and at pressures up to 28 MPa. The instrument and the measuring procedure were described in detail earlier by Hnedkovsky et al.,<sup>15</sup> and only the most salient features will be given here.

The core of the calorimeter is a temperature-controlled massive block housing two identical cells from the platinum–iridium tubing of 2 mm o.d. equipped with a wire heater wound around the tube and with the RTDs detecting the temperature rise of the heated fluid compared to the block. The ratio of specific heat capacities,  $c_p/c_{p,w}$ , is related to the heating powers in the measuring cell as follows

$$c_p/c_{p,w} = (\rho_w/\rho)_{\text{SL}} \{ 1 + f(P - P_w)/P_w \} \quad (7)$$

where  $(\rho_w/\rho)_{\text{SL}}$  is the ratio of water and solution densities at the temperature of the sample loop (typically 298 K) and the pressure of the experiment and where  $f$  is the correction factor for heat losses. The electric powers,  $P$  and  $P_w$ , keep the identical temperature rise,  $\Delta T_{\text{exp}} \cong 2$  K, when the sample solution and water are flowing alternately through the measuring cell. A second (reference) cell connected in series with the measuring cell is used to equilibrate the temperature bridge and to compensate for the flow rate and temperature fluctuations in the calorimeter. The heat loss correction factor,  $f$ , was determined by changing the water base flow rate,  $F_w$ , in the sample cell to mimic a change in heat capacity and by measuring the corresponding change in the heating input. The resulting values of  $f = \Delta F P_w / (\Delta P F_w)$  typically varied from 1.02 (323 K) to 1.09 (623 K) and were determined with an uncertainty of about 2.5%.

The temperature reported for calorimetric measurements represents the average temperature before (assumed to be equal to the temperature of the block,  $T_{\text{block}}$ ) and after the cell heater,  $T = T_{\text{block}} + 0.5\Delta T_{\text{exp}}$ . The stability of the block temperature (0.02 K) is insured by a system of heated, concentric jackets and lids that also serve for preheating of fluids coming into the block. A 500  $\Omega$  secondary standard of Burns, calibrated by the manufacturer against the IPTS 90 standard, was used to measure the temperature of the block. Considering the possibility of

temperature gradients at high temperatures, the uncertainty in temperature determination is estimated to be 0.1 K near the upper temperature limit.

A sample loop with an internal volume of approximately 20 cm<sup>3</sup> is placed in a water bath thermostat (298 K), filled with the solution of interest, and pre-pressurized to the experimental pressure. The sample is then injected into the calorimeter by inserting the loaded sample loop into the stream of water between the reference and measuring cells. A high-pressure pump, working at a constant volumetric flow rate, was used to supply the base flow ( $F_w = 1.8$  cm<sup>3</sup> min<sup>-1</sup>) to the calorimeter. The pressure was maintained constant within 0.05 MPa by a back-pressure regulator placed at the end of the stream, similar to that for the densitometer. The pressure in the system was measured with a Bourdon-type pressure gauge (Heise, CM-63961) with an accuracy of 0.1 MPa.

The apparent molar heat capacities of phosphoric acid solutions were determined for six temperatures between 323 and 623 K and at two pressures, close to the saturation pressure of water and near 28 MPa. For each temperature and pressure, measurements were performed at least at four different concentrations between 0.05 and 0.8 mol kg<sup>-1</sup>, with typically two data points per sample. This leads to 106 new data points for the determination of  $C_{p,\phi}^{\text{exp}}$ . For all conditions of  $T$  and  $p$ ,  $C_{p,\phi}^{\text{exp}}$  is increasing linearly with concentration at temperatures below 573 K; the evolution is nonlinear at the two highest temperatures. The error in the apparent molar heat capacity is calculated as a propagation of the uncertainty in the heat capacity ratio that was obtained as a statistical estimate, taking into account the instabilities of  $P$  and  $P_w$  as well as uncertainties in  $(\rho)_{\text{SL}}$  and in the  $f$  factor (see eq 7). In addition, the systematic error due to the uncertainty in the sample concentration is also taken into consideration. A detailed description of the error estimation is given by Slavik et al.<sup>16</sup> The experimental heat capacity ratios, apparent molar heat capacities, and their estimated errors are integrally available in the Supporting Information.

## Results

**Corrections for Ionization.** Phosphoric acid as a weak electrolyte undergoes partial ionization in aqueous solutions. Only the first-degree dissociation was considered here since the higher-degree dissociation can be neglected, as indicated in the Introduction. The mass balance for the reaction in eq 1 is given by

$$m(\text{H}^+) = m(\text{H}_2\text{PO}_4^-) = \alpha \times m \quad (8)$$

$$m(\text{H}_3\text{PO}_4) = (1 - \alpha)m \quad (9)$$

where  $m$  is the stoichiometric molality and where  $\alpha$  is the degree of dissociation of the acid, which is obtained from solving the equation

$$K_{\text{dis}} = \frac{\alpha^2 m \gamma_{\pm}^2}{(1 - \alpha) \gamma_u} \quad (10)$$

At all experimental conditions, we considered the activity coefficient of uncharged acid,  $\gamma_u$ , to be equal to unity, which is a reasonable approximation for a nonelectrolyte species in diluted solutions. Mean activity coefficients of the univalent



ions  $H^+$  and  $H_2PO_4^-$  were estimated from the extended Debye–Hückel limiting law proposed by Pitzer<sup>17</sup>

$$\ln \gamma_{\pm} = -A_{\Phi} \left[ \frac{(\alpha \times m)^{1/2}}{1 + 1.2(\alpha \times m)^{1/2}} + (2/1.2) \ln(1 + 1.2(\alpha \times m)^{1/2}) \right] \quad (11)$$

where  $A_{\Phi}$  is the Debye–Hückel slope for the osmotic coefficient, taken from the formulation of Archer and Wang,<sup>18</sup> which is based on the fundamental equation of state for water by Hill.<sup>14</sup> Activity coefficients calculated with the above approximations can be compared with the values reported by Holmes and Mesmer<sup>19</sup> that are based on isopiestic measurements of  $H_3PO_4$  (aq). In the case of the uncharged acid, the maximum difference in the activity coefficients was found to be 10% at the highest temperature and molality; the differences for  $\gamma_{\pm}$  were up to 15% and as low as just a few percent in most cases, which is sufficiently accurate for evaluating the corrections for ionization.

The nominal apparent molar properties,  $V_{\Phi}^{\text{exp}}$  or  $C_{p,\Phi}^{\text{exp}}$ , resulting from the experiments are a sum of contributions of undissociated and ionized species. In addition, a chemical relaxation term must be considered in case of the apparent molar heat capacity,<sup>20,21</sup> representing the thermal shift associated with the change in equilibrium composition during the measurement of the solution heat capacity

$$V_{\Phi}^{\text{exp}} = (1 - \alpha)V_{\Phi}(\text{H}_3\text{PO}_4) + \alpha[V_{\Phi}(\text{H}^+) + V_{\Phi}(\text{H}_2\text{PO}_4^-)] \quad (12)$$

$$C_{p,\Phi}^{\text{exp}} = (1 - \alpha)C_{p,\Phi}(\text{H}_3\text{PO}_4) + \alpha[C_{p,\Phi}(\text{H}^+) + C_{p,\Phi}(\text{H}_2\text{PO}_4^-)] + \Delta H_{\text{dis}} \left( \frac{\partial \alpha}{\partial T} \right)_p \quad (13)$$

where  $\Delta H_{\text{dis}}$  corresponds to the enthalpy change during the first-degree dissociation. The concentration dependence of the contributions of the ionized part of the acid was consistently estimated from the Pitzer's modification<sup>17</sup> of the Debye–Hückel law

$$V_{\Phi}(\text{H}^+) + V_{\Phi}(\text{H}_2\text{PO}_4^-) = V_s^{\circ}(\text{H}^+) + V_s^{\circ}(\text{H}_2\text{PO}_4^-) + (A_V/1.2) \ln(1 + 1.2(\alpha \times m)^{1/2}) \quad (14)$$

$$C_{p,\Phi}(\text{H}^+) + C_{p,\Phi}(\text{H}_2\text{PO}_4^-) = C_{p,s}^{\circ}(\text{H}^+) + C_{p,s}^{\circ}(\text{H}_2\text{PO}_4^-) + (A_J/1.2) \ln(1 + 1.2(\alpha \times m)^{1/2}) \quad (15)$$

$$\Delta H_{\text{dis}} = H_s^{\circ}(\text{H}^+) + H_s^{\circ}(\text{H}_2\text{PO}_4^-) + (A_L/1.2) \ln(1 + 1.2(\alpha \times m)^{1/2}) - H_s^{\circ}(\text{H}_3\text{PO}_4) \quad (16)$$

with  $A_V$ ,  $A_J$ , and  $A_L$  being the appropriate Debye–Hückel slopes for volume, heat capacity, and enthalpy, respectively, calculated again from the formulation by Archer and Wang.<sup>18</sup> Standard state properties  $V_s^{\circ}$ ,  $C_{p,s}^{\circ}$ , and  $H_s^{\circ}$  in eqs 14–16, as well as equilibrium constants,  $K_{\text{dis}}$  (eq 2), were calculated in an iterative process (see the next paragraph). In the first iteration, they were obtained from the revised HKF model<sup>2</sup> using the SUPCRT92 software package.<sup>1</sup> Then, the degree of dissociation,  $\alpha$ , was evaluated from the nonlinear combination of eqs 10 and 11. It was followed by calculation of the values of the apparent molar properties,  $V_{\Phi}(\text{H}_3\text{PO}_4)$  and  $C_{p,\Phi}(\text{H}_3\text{PO}_4)$ , of the molecular acid by combination of eqs 12–16. Setting  $Y_s^{\circ}(\text{H}^+) = 0$  for all properties and conditions follows the standard hydrogen ion convention adopted in SUPCRT92 and also in this work. The

standard state for aqueous species was that of unit activity in a hypothetical 1 mol  $\text{kg}^{-1}$  solution referenced to infinite dilution.

**Extrapolations to Infinite Dilution and Refinement of Ionization Corrections.** Corrected values of the apparent molar properties,  $Y_{\Phi}(\text{H}_3\text{PO}_4)$  ( $X = V, C_p$ ), were extrapolated to infinite dilution using weighted regression with a polynomial equation

$$Y_{\Phi}(\text{H}_3\text{PO}_4) = Y_s^{\circ}(\text{H}_3\text{PO}_4) + b(1 - \alpha)m + c[(1 - \alpha)m]^2 \quad (17)$$

where  $Y_s^{\circ}(\text{H}_3\text{PO}_4)$  is the standard molar volume or the standard molar heat capacity of the molecular (undissociated) acid. The weights of  $Y_{\Phi}(\text{H}_3\text{PO}_4)$  were set according to  $1/\sigma^2 Y_{\Phi}^{\text{exp}}$ , with  $\sigma Y_{\Phi}^{\text{exp}}$  being the expected error in an apparent molar property, estimated statistically from uncertainties in different input quantities, as indicated above. We did not find it useful to consider the error increase due to the corrections for ionization that are relatively small and well determined in the weights assignment.

The extrapolated values of the standard molar properties obtained in the first iteration were used for the refinement of the ionization and relaxation corrections through an improved calculation of  $K_{\text{dis}}$ ,  $V_s^{\circ}$ ,  $C_{p,s}^{\circ}$ , and  $H_s^{\circ}$  in eqs 10 and 14–16. Starting with the second iteration, the Sedlbauer–O'Connell–Wood<sup>6</sup> (SOCW) thermodynamic model (described below) was used for this purpose instead of the HKF model. The newly corrected data lead to new extrapolations, etc. Three iterations were needed until we reached stable values of the calculated corrections and hence of the extrapolated standard molar volumes and heat capacities, as well as of the parameters of the SOCW model. It should be noted that our corrections compare well with those obtained by Sharygin et al.<sup>22</sup> for the apparent molar heat capacity of  $H_3PO_4$ (aq) at high temperatures, although we used a different approach for evaluating the corrections. Final parameters of eq 17 for the experimental temperatures and pressures are summarized in Table 1; only parameters significant within their 95% confidence limits were accepted and are listed in the table. In most cases, the corrected data for the apparent molar volumes did not significantly change with concentration, and the concentration dependence was linear for the corrected apparent molar heat capacities. The values of the apparent molar properties at infinite dilution, obtained by an extrapolation without any corrections, are also listed for comparison in parentheses. They document to what extent the  $V_s^{\circ}$  and  $C_{p,s}^{\circ}$  values are affected by the ionization and relaxation effects. The errors,  $\sigma Y_s^{\circ}$ , are statistical deviations of the parameter obtained during the regression, and SD is the standard deviation of the fit, reflecting the data scatter.

The corrections evaluated from the HKF and from the SOCW models in the first and in the other iterations, respectively, agreed semiquantitatively in most cases, with larger differences observed at high pressures and at high temperatures. The maximum degree of ionization for our solutions was found to be 26% at 298 K and 0.1 mol  $\text{kg}^{-1}$  and decreased with temperature and concentration. In the case of  $V_{\Phi}(\text{H}_3\text{PO}_4)$ , this brought a maximum correction of 4.2  $\text{cm}^3 \text{mol}^{-1}$ , corresponding to an almost 10% increase of the  $V_{\Phi}(\text{H}_3\text{PO}_4)$  value at 298 K and the lowest concentration compared to the experimental value,  $V_{\Phi}^{\text{exp}}$ . A 12% ionization at a molality of 0.8 mol  $\text{kg}^{-1}$  and the same temperature resulted in a 1.8  $\text{cm}^3 \text{mol}^{-1}$  correction. At higher temperatures, the maximum degrees of ionization (corresponding to 0.1 mol  $\text{kg}^{-1}$  solutions) and respective volumetric corrections were 18% and 3.7  $\text{cm}^3 \text{mol}^{-1}$  at 373 K, 9% and 3.6  $\text{cm}^3 \text{mol}^{-1}$  at 473 K, and 3% and 3.4  $\text{cm}^3 \text{mol}^{-1}$  at 573 K. The

**TABLE 1: Parameters of Equation 17, Allowing One to Obtain the Standard Molar Volume and the Standard Molar Heat Capacity of H<sub>3</sub>PO<sub>4</sub>(aq)**

$T$ K	$p$ MPa	data points, concentrations <sup>a</sup>	$V_s^{\circ}(V_{s,nc}^{\circ})^b$ cm <sup>3</sup> mol <sup>-1</sup>	$\sigma V_s^{\circ}$ cm <sup>3</sup> mol <sup>-1</sup>	$b$ cm <sup>3</sup> mol <sup>-2</sup> kg	$c$ cm <sup>3</sup> mol <sup>-3</sup> kg <sup>2</sup>	SD <sup>c</sup> cm <sup>3</sup> mol <sup>-1</sup>
298.15	0.1	8 (5)	47.5 (43.8)	0.1	—	—	0.1
373.10	10.23	16 (5)	49.3 (46.4)	0.1	—	—	0.3
423.13	1.52	12 (4)	48.8 (46.0)	0.1	—	—	0.3
423.14	10.38	14 (5)	48.9 (46.0)	0.2	—	—	0.6
473.30	1.95	8 (4)	46.4 (43.3)	0.1	—	—	0.3
523.20	4.51	11 (4)	40.0 (35.9)	0.2	—	—	0.7
573.15	9.93	11 (4)	14.4 (11.9)	1.8	6.85	—	1.2
298.24	27.97	4 (2)	47.7 (43.9)	0.1	—	—	0.1
423.15	28.37	12 (4)	49.1 (46.3)	0.1	—	—	0.3
473.11	28.51	9 (4)	47.3 (44.7)	0.2	—	—	0.7
523.23	27.25	12 (4)	43.0 (39.7)	0.2	—	—	0.9
573.19	27.03	17 (5)	30.0 (27.4)	0.6	3.06	—	0.8

$T$ K	$p$ MPa	data points, concentrations <sup>a</sup>	$C_{p,s}^{\circ}(C_{p,s,nc}^{\circ})^b$ J K <sup>-1</sup> mol <sup>-1</sup>	$\sigma C_{p,s}^{\circ}$ J K <sup>-1</sup> mol <sup>-1</sup>	$b$ J K <sup>-1</sup> mol <sup>-2</sup> kg	$c$ J K <sup>-1</sup> mol <sup>-3</sup> kg <sup>2</sup>	SD <sup>c</sup> J K <sup>-1</sup> mol <sup>-1</sup>
322.65	1.8	8 (4)	114.2 (107.0)	1.4	3.4	—	1.0
423.67	10.3	8 (4)	148.0 (146.1)	1.6	4.3	—	1.0
473.64	10.3	8 (4)	131.5 (131.9)	2.4	17.6	—	1.2
523.34	10.5	12 (4)	81.8 (86.0)	2.7	26.8	—	1.8
573.05	12.1	10 (5)	-154.4 (-144.6)	8.0	52.6	—	6.2
623.44	20.5	8 (5)	-2116 (-2116)	117	2105	-1139	39
322.66	28	8 (4)	127.6 (118.6)	5.7	-3.0	—	3.8
423.62	28.6	9 (4)	157.6 (155.5)	4.8	-6.0	—	3.0
473.65	28.4	12 (4)	148.1 (148.1)	1.4	9.2	—	1.4
523.32	29.4	10 (4)	96.6 (101.7)	8.4	50.5	—	4.9
573.06	28	8 (5)	-14.3 (1.3)	6.7	171	-122	2.6
623.45	27.7	5 (5)	-649 (-635)	36	458	-237	14

<sup>a</sup> Total number of data points (number of concentrations). <sup>b</sup> Calculated from non-corrected apparent molar property. <sup>c</sup> Standard deviation of the fit.

situation is more complex in the case of  $C_{p,\Phi}(\text{H}_3\text{PO}_4)$  where the positive correction of ionization decreasing with temperature is offset at higher temperatures by a negative contribution of the chemical relaxation term, which is growing with temperature. As a result, the corrections are generally noticeable at the lowest temperatures (due to ionization) and at the highest temperatures and pressures (due to chemical relaxation): up to 11 J K<sup>-1</sup> mol<sup>-1</sup> at 323 K, 3 J K<sup>-1</sup> mol<sup>-1</sup> at 423 K, -5 J K<sup>-1</sup> mol<sup>-1</sup> at 523 K, and -11 J K<sup>-1</sup> mol<sup>-1</sup> at 623 K (all correspond to a target concentration of 0.1 mol kg<sup>-1</sup> and a pressure of 28 MPa). At conditions where heat capacities become strongly negative (623 K and 20 MPa in our case), the ionization correction is not, however, quite negligible, despite the low value of  $\alpha$ , since the heat capacity of the ion is very high in its absolute value. Then, the two corrections can compensate for each other, as is apparent in Table 1. The complete database of our experimental results with the calculated degrees of dissociation,  $\alpha$ , and the apparent molar properties corrected for ionization is available as Supporting Information.

**Correlation Model.** One of the objectives of this paper is to provide an improved model for calculating the standard thermodynamic properties of both molecular and ionized acetic acid as a function of temperature and pressure. The possibility to calculate the equilibrium constant for the first-degree dissociation of H<sub>3</sub>PO<sub>4</sub>(aq) (eqs 1 and 2) at superambient conditions is of particular interest. The best known representation for these species so far is available with the revised Helgeson–Kirkham–Flowers (HKF) model,<sup>2</sup> mentioned already in connection with evaluation of the corrections for ionization. Parameters of the HKF model were obtained from the thermodynamic data at ambient conditions and from ionization constants to 573 K (Mesmer and Baes<sup>23</sup> and Read<sup>24</sup>); no high-temperature thermodynamic data relating to individual species were employed by Helgeson and collaborators. Another reason for improvement

is the empirical nature of the HKF equations for aqueous nonelectrolytes, which does not allow for quantitative description of the derivative properties (standard molar volumes and heat capacities) at high temperatures. Considering the handicaps of the HKF approach, we decided to apply the Sedlbauer–O’Connell–Wood (SOCW) model, which was already shown to be sufficiently versatile and reliable for simultaneous correlation of different standard molar properties of ions as well as nonelectrolytes in a wide range of conditions.<sup>7,10,25,26</sup> A detailed description of the SOCW model equations was given elsewhere,<sup>6</sup> and only the most important features will be noted here.

The development of this model started with a relationship between the spatial integral of the infinite-dilution solute–water direct correlation function,  $C_{sw}^{\circ}$ , and dimensionless parameter,  $A_{sw}^{\circ}$ , called the modified Krichevskii parameter<sup>9</sup>

$$1 - C_{sw}^{\circ} = \frac{V_s^{\circ}}{\kappa_w RT} = A_{sw}^{\circ} \quad (18)$$

where  $\kappa_w$  is the compressibility of the water solvent. The  $A_{sw}^{\circ}$  function is known to be well-behaved in the critical region of water and was therefore chosen as a basis for correlations extending to these conditions. Sedlbauer et al.<sup>6</sup> formulated the model for standard molar volume,  $V_s^{\circ}$ , consisting of three parts. The first corresponds to insertion of a point mass into water, the second term reflects the cavity-formation effect of solute particle, which is supposed to scale with the molar volume of water, and the third empirical part is responsible for solute–water interaction

$$V_s^{\circ} = (1 - z)\kappa_w RT + d(V_w - \kappa_w RT) + \kappa_w RT \rho_w (a + b[\exp(\vartheta \rho_w) - 1] + c \exp(\theta/T) + \delta[\exp(\lambda \rho_w) - 1]) \quad (19)$$

Universal constants that appear in eq 19 are  $v = 0.005 \text{ m}^3 \text{ kg}^{-1}$ ,  $\lambda = -0.01 \text{ m}^3 \text{ kg}^{-1}$ , and  $\theta = 1500 \text{ K}$ ;  $a$ ,  $b$ ,  $c$ , and  $d$  are adjustable parameters, specific for each solute, and  $z$  is the charge of a particle ( $z = 0$  for neutral molecules,  $z \geq 1$  for cations, and  $-z \geq 1$  for anions). The  $(1 - z)$  multiplication factor is needed in order to comply with the hydrogen convention for aqueous ions, which requires  $Y_s^{\circ}(\text{H}^+) = 0$ . Using  $a = b = c = d = \delta = 0$  for  $\text{H}^+(\text{aq})$  would leave the point-mass term ( $\kappa_w RT$ ) in the equation; it has to be removed by formal assignment of both point-mass terms in a 1/1 electrolyte/anion ratio. The parameter  $\delta$  is determined depending on the charge of the solute; for nonelectrolytes with its charge equal to zero,  $\delta = 0.35a$ , for anions,  $\delta = -0.645 \text{ m}^3 \text{ kg}^{-1}$ , and for cations,  $\delta = 0 \text{ m}^3 \text{ kg}^{-1}$ . Again, the asymmetric choice of  $\delta$  for cations and anions is dictated by the hydrogen convention.

The resulting equation for the standard molar volume (eq 19) is integrated to obtain the Gibbs energy of hydration. For the hydration process, the integration proceeds from an ideal gas, standard state at temperature  $T$  and standard pressure  $p_0 = 0.1 \text{ MPa}$  to the standard state of infinite dilution at  $T$ ,  $p$ .

$$\Delta_{\text{hyd}}G^{\circ} = RT \ln(p/p_0) + \int_0^p \left( V_s^{\circ} - \frac{RT}{p} \right) dp + G_s^{\text{corr}} \quad (20)$$

The correction function,  $G_s^{\text{corr}}$ , is used at subcritical conditions ( $T < T_c = 647.1 \text{ K}$ ) where the two-phase boundary is crossed in the course of integration from  $p_0$  to  $p$ . The value of this correction is monotonously decreasing with increasing temperature; it is equal to zero at the critical temperature of water and (by definition) equal to zero at supercritical conditions. Using the SOCW equation for  $V_s^{\circ}$ , the hydration Gibbs energy is

$$\begin{aligned} \Delta_{\text{hyd}}G^{\circ} = & (1 - z)RT \ln[\rho_w RT/p_0] + d(G_w - G_w^{\text{ig}} - \\ & RT \ln[\rho_w RT/(p_0 M_w)]) + RT\{(a + c \exp(\theta/T) - b - \delta)\rho_w + \\ & b/\vartheta[\exp(\vartheta\rho_w) - 1] + \delta/\lambda[\exp(\lambda\rho_w) - 1]\} + G_s^{\text{corr}} \quad (21) \end{aligned}$$

where  $G_w$  is the molar Gibbs energy of water,  $G_w^{\text{ig}}$  is the same property in an ideal gas, standard state, and  $M_w$  is molar mass of water. We adopted the following functional form of the correction term<sup>6</sup>

$$\begin{aligned} G_s^{\text{corr}} = & g(T^2 - T_c^2)/2 + (T - T_c)(e - gT_c) + \\ & e(\Theta - T_c) \ln \frac{T - \Theta}{T_c - \Theta} - T \left( g(T - T_c) + (e - g\Theta) \frac{T_c}{\Theta} \ln \frac{T}{T_c} + \right. \\ & \left. e \frac{\Theta - T_c}{\Theta} \ln \frac{T - \Theta}{T_c - \Theta} \right) \quad (22) \end{aligned}$$

where  $e$  and  $g$  are two additional adjustable parameters and where  $\Theta = 228 \text{ K}$ . The standard entropy of hydration can then be obtained by temperature derivation of  $\Delta_{\text{hyd}}G_s^{\circ}$

$$\Delta_{\text{hyd}}S^{\circ} = - \left( \frac{\partial \Delta_{\text{hyd}}G^{\circ}}{\partial T} \right)_p \quad (23)$$

The standard chemical potential,  $G_s^{\circ}$ , is calculated by adding the Gibbs energy of a solute in an ideal gas, standard state at  $p_0 = 0.1 \text{ MPa}$  to  $\Delta_{\text{hyd}}G_s^{\circ}$

$$G_s^{\circ} = \Delta_{\text{hyd}}G^{\circ} + G_s^{\text{ig}} \quad (24)$$

The term  $G_s^{\text{ig}}$  is defined here as

$$\begin{aligned} G_s^{\text{ig}} = & G_{s,\text{f}}^{\text{ig}}[T_r] + (G_s^{\text{ig}}[T] - G_s^{\text{ig}}[T_r]) = \\ & G_{s,\text{f}}^{\text{ig}}[T_r] + (T_r - T)S_s^{\text{ig}}[T_r] + (H_s^{\text{ig}}[T] - H_s^{\text{ig}}[T_r]) - \\ & T(S_s^{\text{ig}}[T] - S_s^{\text{ig}}[T_r]) \quad (25) \end{aligned}$$

where  $G_{s,\text{f}}^{\text{ig}}$  and  $S_s^{\text{ig}}$  are the Gibbs energy of formation and the entropy of a solute in an ideal gas, standard state at  $T_r = 298.15 \text{ K}$ , respectively. The enthalpy and entropy differences can be obtained as temperature integrals of the ideal gas heat capacity. All of these properties can be evaluated from spectroscopic data.

It is a common practice to constrain calculated standard chemical potentials of aqueous solutes by experimental values of standard thermodynamic properties at some reference conditions, typically  $T_r = 298.15 \text{ K}$  and  $p_r = 0.1 \text{ MPa}$ , where they are usually known with good accuracy. In this context, it is possible to write the Gibbs energy of hydration<sup>26</sup> as

$$\begin{aligned} \Delta_{\text{hyd}}G^{\circ} = & \Delta_{\text{hyd}}G^{\circ,\text{lit}}[T_r, p_r] + (T_r - T)\Delta_{\text{hyd}}S^{\circ,\text{lit}}[T_r, p_r] - \\ & \Delta_{\text{hyd}}G^{\circ,\text{SOCW}}[T_r, p_r] - (T_r - T)\Delta_{\text{hyd}}S^{\circ,\text{SOCW}}[T_r, p_r] + \\ & \Delta_{\text{hyd}}G^{\circ,\text{SOCW}}[T, p] \quad (26) \end{aligned}$$

where the quantities with superscripts lit and SOCW are taken as recommended values from the literature and calculated from the SOCW model (eqs 21 and 23), respectively. After some rearrangement, the previous two equations then transform to

$$\begin{aligned} G_s^{\circ} = & G_s^{\circ,\text{lit}}[T_r, p_r] - (T - T_r)S_s^{\circ,\text{lit}}[T_r, p_r] + \Delta H_s^{\text{ig}} - T\Delta S_s^{\text{ig}} - \\ & (\Delta_{\text{hyd}}G^{\circ,\text{SOCW}}[T_r, p_r] - (T - T_r)\Delta_{\text{hyd}}S^{\circ,\text{SOCW}}[T_r, p_r]) + \\ & \Delta_{\text{hyd}}G^{\circ,\text{SOCW}}[T, p] \quad (27) \end{aligned}$$

where  $G_s^{\circ,\text{lit}} = G_{s,\text{f}}^{\text{ig}} + \Delta_{\text{hyd}}G^{\circ,\text{lit}}$  and  $S_s^{\circ,\text{lit}} = S_s^{\text{ig}} + \Delta_{\text{hyd}}S^{\circ,\text{lit}}$  are available from the literature at  $T_r$  and  $p_r$ ;  $\Delta H_s^{\text{ig}}$  and  $\Delta S_s^{\text{ig}}$  are the changes in the ideal gas enthalpy and entropy between  $T_r$  and  $T$  introduced in eq 25. The standard derivative properties,  $C_{p,s}^{\circ}$  and  $V_s^{\circ}$ , can be obtained as derivatives of  $G_s^{\circ}$ , expressed by eq 27

$$C_{p,s}^{\circ} = -T \left( \frac{\partial^2 G_s^{\circ}}{\partial T^2} \right)_p \quad (28)$$

$$V_s^{\circ} = \left( \frac{\partial G_s^{\circ}}{\partial p} \right)_T \quad (29)$$

The SOCW model requires six species-specific parameters that can be adjusted by a simultaneous correlation of an array of experimental data. For this purpose, we have employed the results on  $V_s^{\circ}(\text{H}_3\text{PO}_4)$  and  $C_{p,s}^{\circ}(\text{H}_3\text{PO}_4)$  obtained in this study, standard molar heat capacities from Sharygin et al.<sup>22</sup> (six values between 303 and 623 K and near 28 MPa that we have corrected for dissociation), and the first-degree ionization constants of phosphoric acid from the potentiometric measurements by Mesmer and Baes<sup>23</sup> at 573 K along the saturation line of water and from the conductivity results by Read<sup>24</sup> at 473 K and 200 MPa. We have also included the standard molar volumes and heat capacities of  $\text{H}_3\text{PO}_4(\text{aq})$  and  $\text{H}_2\text{PO}_4^-(\text{aq})$  at 298 K and 0.1 MPa reported by Larson et al.<sup>21</sup> A few other data available in literature at or close to ambient conditions were not used for the following reasons: (i) the model is already constrained at 298 K and 0.1 MPa by the values of the standard chemical potential and the standard molar entropy recommended by Wagman et al.<sup>27</sup> and also conditioned by the  $C_{p,s}^{\circ}$  and  $V_s^{\circ}$  values of Larson and collaborators taken with a high weight and (ii)

**TABLE 2: Parameters  $a$ – $g$  of the SOCW Model Obtained from the Simultaneous Correlation of the Standard Derivative Properties with the Thermodynamic Constants of Dissociation and the Literature Values of  $G_s^{\text{ol, lit}}$  and  $S_s^{\text{ol, lit}}$  at 298 K and 0.1 MPa<sup>a</sup>**

solute	$G_s^{\text{ol, lit}}$	$S_s^{\text{ol, lit}}$	$10^3 a$	$10^4 b$	$10^6 c$	$d$	$10e$	$g$
H <sub>3</sub> PO <sub>4</sub> (aq)	−1142.65	158.99	−2.8870	−0.38470	−9.2321	3.3420	8.4448	−0.22984
H <sub>2</sub> PO <sub>4</sub> <sup>−</sup> (aq)	−1130.27	90.37	−669.04	1.4126	−11.789	2.0470	15.200	−0.63533

<sup>a</sup> Units:  $G_s^{\text{ol, lit}}$  (kJ mol<sup>−1</sup>);  $S_s^{\text{ol, lit}}$  (J K<sup>−1</sup> mol<sup>−1</sup>);  $a$ ,  $b$ , and  $c$  (m<sup>3</sup> kg<sup>−1</sup>);  $e$  (J K<sup>−1</sup> mol<sup>−1</sup>);  $g$  (J K<sup>−2</sup> mol<sup>−1</sup>). <sup>b</sup> Wagman et al.<sup>27</sup>

**TABLE 3: Standard Thermodynamic Properties of H<sub>3</sub>PO<sub>4</sub>(aq) and H<sub>2</sub>PO<sub>4</sub><sup>−</sup>(aq) as a Function of Temperature at the Saturation Pressure of Water and at 100 MPa/200 MPa Isobars, Calculated from the SOCW Model**

$T$ (K)	$p$ (MPa)	$G_s^{\text{ol, a}}$ kJ mol <sup>−1</sup>	$S_s^{\text{ol, a}}$ J K <sup>−1</sup> mol <sup>−1</sup>	$V_s^{\text{ol, a}}$ cm <sup>3</sup> mol <sup>−1</sup>	$C_{p,s}^{\text{ol, a}}$ J K <sup>−1</sup> mol <sup>−1</sup>	$G_s^{\text{ol, b}}$ kJ mol <sup>−1</sup>	$S_s^{\text{ol, b}}$ J K <sup>−1</sup> mol <sup>−1</sup>	$V_s^{\text{ol, b}}$ cm <sup>3</sup> mol <sup>−1</sup>	$C_{p,s}^{\text{ol, b}}$ J K <sup>−1</sup> mol <sup>−1</sup>
298.15	$p^{\text{sat}}$	−1142.6	159.0	47.8	98	−1130.3	90.4	30.9	−33
373.15	$p^{\text{sat}}$	−1155.6	185.3	49.0	133	−1137.1	93.4	26.9	19
423.15	$p^{\text{sat}}$	−1165.2	202.8	48.6	143	−1141.8	92.3	18.5	−50
473.15	$p^{\text{sat}}$	−1175.7	218.5	46.6	132	−1146.1	79.1	0.8	−219
523.15	$p^{\text{sat}}$	−1186.9	229.5	39.6	61	−1149.3	42.0	−40.2	−641
573.15	$p^{\text{sat}}$	−1198.2	226.5	13.0	−309	−1149.8	−55.9	−160	−2266
623.15	$p^{\text{sat}}$	−1208.6	120.1	−222.8	−8568	−1142.7	−564.2	−1105	−34592
298.15	100	−1137.9	154.7	46.5	132	−1127.0	90.1	34.8	13
373.15	100	−1150.7	184.5	48.2	140	−1134.1	101.8	32.3	66
423.15	100	−1160.4	203.1	48.7	156	−1139.4	108.7	27.9	38
473.15	100	−1171.0	221.1	48.8	166	−1144.9	109.8	20.2	−24
523.15	100	−1182.5	237.9	48.3	167	−1150.2	103.0	7.3	−119
573.15	100	−1194.8	252.8	46.5	158	−1155.0	86.5	−14.2	−253
623.15	100	−1207.7	265.3	42.4	138	−1158.7	58.3	−50.7	−433
298.15	200	−1133.3	150.6	45.5	155	−1123.3	90.7	37.5	36
373.15	200	−1145.9	183.1	47.2	145	−1130.7	107.1	35.6	91
423.15	200	−1155.5	202.2	47.9	159	−1136.3	118.0	32.6	77
473.15	200	−1166.1	220.7	48.4	171	−1142.4	124.8	28.0	41
523.15	200	−1177.6	238.3	48.8	178	−1148.7	126.3	20.9	−13
573.15	200	−1189.9	254.7	48.9	181	−1155.0	122.3	10.8	−77
623.15	200	−1203.0	269.8	48.7	180	−1160.9	113.1	−3.6	−146

<sup>a</sup> Molecular H<sub>3</sub>PO<sub>4</sub>(aq). <sup>b</sup> Anionic H<sub>2</sub>PO<sub>4</sub><sup>−</sup>(aq).

we wished not to overweight the near-ambient region in the correlation in order to provide a model applicable in a wide range of conditions (up to the critical temperature of water and 200 MPa). The minimized objective function was

$$F = \sum_{i=1}^O \left( \frac{K_{\text{dis}}^{\text{exp}} - K_{\text{dis}}^{\text{calcd}}}{\sigma K_{\text{dis}}} \right)_i^2 + \sum_{j=1}^P \left( \frac{C_{p,s}^{\text{ol, exp}} - C_{p,s}^{\text{ol, calcd}}}{\sigma C_{p,s}^{\text{ol}}} \right)_k^2 + \sum_{k=1}^Q \left( \frac{V_s^{\text{ol, exp}} - V_s^{\text{ol, calcd}}}{\sigma V_s^{\text{ol}}} \right)_l^2 \quad (30)$$

where superscripts exp and calcd denote the data derived from experiments and values calculated with the SOCW model, respectively. Parameters  $a$ – $g$ , obtained in this way simultaneously for molecular H<sub>3</sub>PO<sub>4</sub>(aq) and for anionic H<sub>2</sub>PO<sub>4</sub><sup>−</sup>(aq), are given in Table 2, along with the literature values<sup>27</sup> of  $G_s^{\text{ol, lit}}[T_r, p_r]$  and  $S_s^{\text{ol, lit}}[T_r, p_r]$  used for constraining the correlation. The heat capacities of H<sub>3</sub>PO<sub>4</sub> and H<sub>2</sub>PO<sub>4</sub><sup>−</sup> in the ideal gas, standard state needed in eq 27 were considered equal because the ideal gas heat capacity change due to structural difference of one hydrogen atom is generally negligible. We could not, however, locate  $C_{p,s}^{\text{ig}}$  for H<sub>3</sub>PO<sub>4</sub> in the literature; instead, we have used  $C_{p,s}^{\text{ig}}$  of H<sub>3</sub>BO<sub>3</sub> represented as a correlation based on the data from the JANAF Tables<sup>28</sup>

$$C_{p,s}^{\text{ig}} = 21.9989 + 0.179237T - 1.17444 \times 10^{-4}T^2 + 3.00843 \times 10^{-8}T^3 \quad (31)$$

This approximation is acceptable, considering that the hydration part of the standard molar heat capacity is adjusted based on experimental results up to high temperatures, and the possible

inaccuracy of  $C_{p,s}^{\text{ig}}$  is therefore hidden in the parameters of the SOCW model. Table 3 lists the values of the standard thermodynamic properties for molecular acid and the H<sub>2</sub>PO<sub>4</sub><sup>−</sup> ion generated from the SOCW model using parameters in Table 2 as a function of temperature and pressure. The listed values for the anion should be considered as approximate since they are not based on any direct experimental data for the derivative properties of phosphate salts. They are obtained exclusively by combining the thermodynamic properties of the molecular acid with those characterizing the dissociation process. It is apparent that the standard chemical potentials of the molecular acid and its anion are relatively close, corresponding to a low value of the dissociation constant  $K_{\text{dis}}$ , and change only moderately with temperature and pressure. Much more important differences between molecular and ionized acid are observed for  $V_s^{\text{ol}}$  and  $C_{p,s}^{\text{ol}}$  where the ion has systematically lower values. Since these two standard derivative properties scale at high temperatures with compressibility and the temperature derivative of expansivity of water, respectively, they are strongly pressure dependent near the upper temperature limit and tend toward minus infinity at the critical point of water. This is well apparent when comparing the temperature variation of  $V_s^{\text{ol}}$  and  $C_{p,s}^{\text{ol}}$  along the saturation line of water with their isobars at 100 and 200 MPa.

Application of a complete thermodynamic model such as the HKF or SOCW may bring some difficulty because of the necessity to use a fundamental equation of state for water, exactly like that during the parameter adjustment, when generating the required thermodynamic properties of a solute. When the target quantity in the application is the standard chemical potential, it is worthwhile to examine also a possibility of adopting a simplified approach based on the observation that the standard molar volumes and heat capacities of aqueous



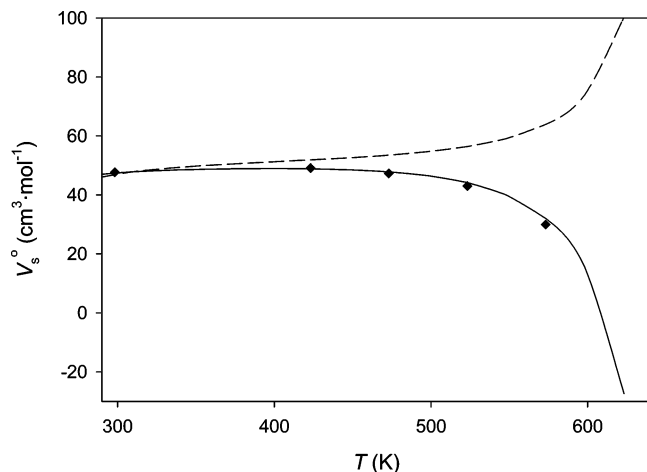


**Figure 1.** Standard molar volumes  $V_s^\circ$  at  $p = 28$  MPa isobar. Filled diamonds, data obtained in this study; full line, SOCW model with parameters from Table 2; dashed line, HKF model with parameters from SUPCRT92.<sup>1</sup>

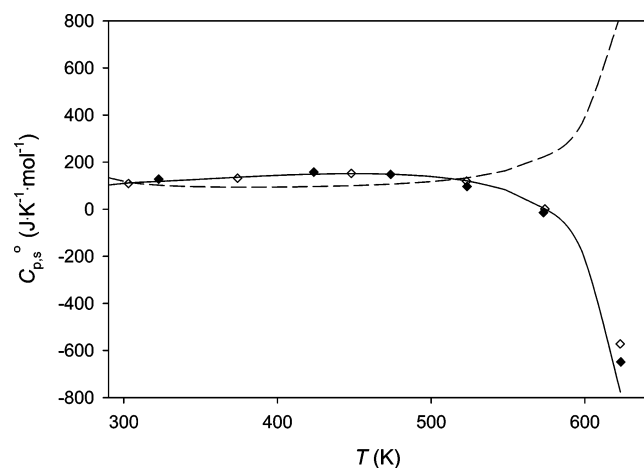


**Figure 2.** Standard molar heat capacities  $C_{p,s}^\circ$  at  $p = 28$  MPa isobar. Filled diamonds, data obtained in this study; open diamonds, data from Sharygin et al.;<sup>22</sup> full line, SOCW model with parameters from Table 2; dashed line, HKF model with parameters from SUPCRT92.<sup>1</sup>

species do not change strongly up to about 450 K. Considering the values of  $C_{p,s}^\circ$  and  $V_s^\circ$  as constant (taken as equal to the values recommended in the literature at  $T_r = 298$  K and  $p_r = 0.1$  MPa), we get the following equation for the standard chemical potential by the simple thermodynamic integration of eqs 28 and 29:

$$G_s^\circ = G_s^{\circ,\text{lit}}[T_r, p_r] - (T - T_r)S_s^{\circ,\text{lit}}[T_r, p_r] + (T - T_r)C_{p,s}^{\circ,\text{lit}}[T_r, p_r] - T \ln(T/T_r)C_{p,s}^{\circ,\text{lit}}[T_r, p_r] + (p - p_r)V_s^{\circ,\text{lit}}[T_r, p_r] \quad (32)$$

## Discussion and Conclusions

**Model Predictions.** The calculations of  $V_s^\circ$  and  $C_{p,s}^\circ$  from the SOCW and HKF models are compared in Figures 1 and 2 with the data resulting from our experiments (and from those of Sharygin et al.<sup>21</sup> for  $C_{p,s}^\circ$ ) along the 28 MPa isobar. The HKF model obviously fails at higher temperatures, producing even a wrong sign of the critical divergence for both standard derivative properties. This is not quite surprising; no experimental results on derivative standard thermodynamic properties such as  $V_s^\circ$  or  $C_{p,s}^\circ$  at high temperatures were included when the HKF parameters were evaluated and then taken over in the SUPCRT92

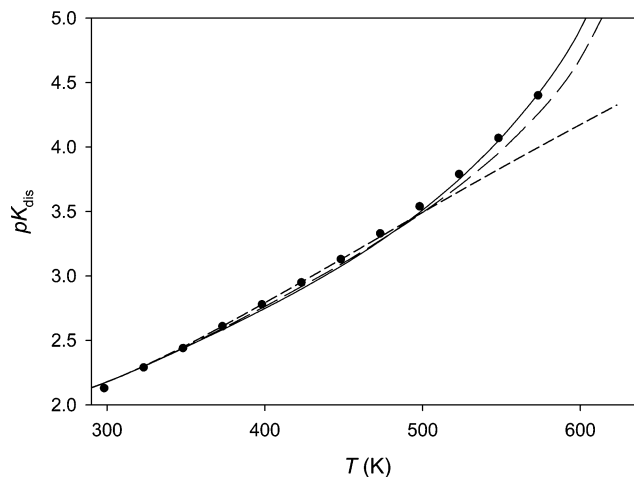


**Figure 3.**  $pK_{\text{dis}} = -\log K_{\text{dis}}$  for the ionization equilibrium (eq 1) at the saturation pressure of water. Filled circles, data from Mesmer and Baes;<sup>23</sup> full line, SOCW model with parameters from Table 2; medium-dashed line, HKF model with parameters from SUPCRT92;<sup>1</sup> short-dashed line, predictions based on eq 32 with the data from refs 21 and 27.

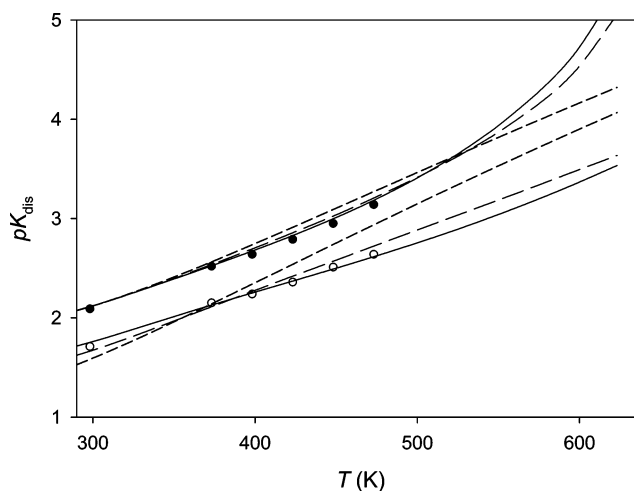


**Figure 4.**  $pK_{\text{dis}} = -\log K_{\text{dis}}$  for the ionization equilibrium (eq 1) at  $p = 20$  and  $p = 200$  MPa isobars. Filled circles, data from Read<sup>24</sup> at 20 MPa; empty circles, data from Read<sup>24</sup> at 200 MPa; full line, SOCW model with parameters from Table 2; medium-dashed line, HKF model with parameters from SUPCRT92;<sup>1</sup> short-dashed line, predictions based on eq 32 with the data from refs 21 and 27.

database. On the other hand, it is known that simultaneous treatment of a large body of experimental data does not bring substantial improvement to the HKF parametrization.<sup>5,25</sup> The problem is mainly in the theoretical drawbacks of the HKF approach, particularly in the interconnection of certain terms, that cannot be circumvented and that prevent one from using the modern approach of multiproperty fitting.

However rough the model approximation of derivative properties is, much of its inaccuracy is, however, attenuated in the course of integration for obtaining the change in the standard chemical potential. This is documented in Figures 3 and 4, displaying  $pK_{\text{dis}} = \Delta_{\text{dis}}G^\circ/(2.303RT)$  for the ionization reaction (eq 1). The  $pK_{\text{dis}}$  values can easily be calculated from the values of  $G_s^\circ$  listed in Table 3. They change between 298 and 623 K from 2.2 to 5.5 along the saturation line of water, while in the same temperature interval, the variation of  $pK_{\text{dis}}$  is between 1.8 and 3.5 at 200 MPa. This reflects the significant drop of the dissociation constant with temperature and an important effect of pressure at high temperatures. Besides the calculation from the SOCW model, Figures 3 and 4 include also the results



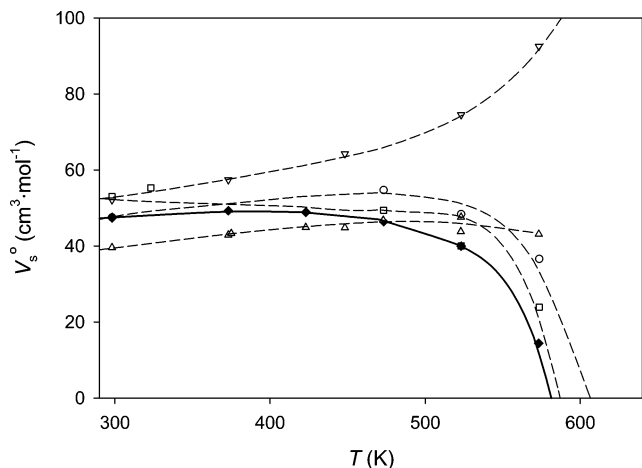


**Figure 5.** Standard molar volumes  $V_s^o$  of inorganic acids resulting from experimental data at pressures below 15 MPa. Filled diamonds, H<sub>3</sub>PO<sub>4</sub>(aq) (this study); empty squares, H<sub>3</sub>AsO<sub>4</sub>(aq) (Perfetti<sup>34</sup>); empty circles, H<sub>3</sub>AsO<sub>3</sub>(aq) (Perfetti<sup>34</sup>); empty triangles, H<sub>3</sub>BO<sub>3</sub>(aq) (Hnedkovsky et al.<sup>29</sup>); filled triangles, H<sub>3</sub>BO<sub>3</sub>(aq) (Ganopolsky et al.<sup>30</sup>); reversed triangles, CH<sub>3</sub>COOH(aq) (Majer et al.<sup>10</sup>). The lines are to lead the eye.

generated from the HKF equations (SUPCRT92) and from eq 32, assuming constant values of  $V_s^o$  and  $C_{p,s}^o$ . In this latter case, the values reported at 298.15 K and 0.1 MPa by Larson et al.<sup>21</sup> were used ( $V_s^{\circ\text{lit}}(\text{H}_3\text{PO}_4) = 48.1 \text{ cm}^3 \text{ mol}^{-1}$ ,  $C_{p,s}^{\circ\text{lit}}(\text{H}_3\text{PO}_4) = 94 \text{ J mol}^{-1} \text{ K}^{-1}$ ,  $V_s^{\circ\text{lit}}(\text{H}_2\text{PO}_4^-) = 31.3 \text{ cm}^3 \text{ mol}^{-1}$ , and  $C_{p,s}^{\circ\text{lit}}(\text{H}_2\text{PO}_4^-) = -34 \text{ J mol}^{-1} \text{ K}^{-1}$ ) in combination with the values of Wagman et al. for  $G_s^{\circ\text{lit}}$  and  $S_s^{\circ\text{lit}}$  (Table 2). Satisfactory predictions (up to 0.1 difference in  $\text{p}K_{\text{dis}}$  units compared to that of the experimental data) are obtained with this simple approximation at about 473 K along the saturation line of water; at higher pressures, this limit decreases to about 390 K at  $p = 200 \text{ MPa}$ . For the HKF equations, the same limits are reached at about 530 K at the saturation pressure and at 440 K at  $p = 200 \text{ MPa}$ . Calculations with the SOCW model stay within the expected experimental uncertainty of the data (up to 0.05  $\text{p}K_{\text{dis}}$  units) at all conditions. It is also expected that extrapolations with the SOCW model outside of the range of the experimental data are reliable at least to the critical region of water because the model accurately describes standard derivative properties to 623 K, and as an implicit feature, it provides correct near-critical scaling.<sup>6</sup>

We conclude that the SOCW model is capable of reliably describing the data resulting from different experimental results for H<sub>3</sub>PO<sub>4</sub>(aq) and H<sub>2</sub>PO<sub>4</sub><sup>-</sup>(aq) and also provides the best extrapolations and estimates of the ionization properties. When developing an accurate model for standard thermodynamic properties applicable in a wide range of conditions, it is desirable to also use the standard derivative properties resulting from volumetric and calorimetric experiments up to high temperatures as input. Finally, the simple thermodynamic integration using eq 32 is a viable option for calculating the standard chemical potentials at conditions not too far removed from ambient (say, up to 400 K).

**Standard Derivative Properties of Strongly Polar Non-electrolytes.** The first experimental evidence of negative, near-critical divergence for standard derivative properties of a nonelectrolyte was reported some 10 years ago in the case of boric acid (Hnedkovsky et al.<sup>29</sup>). Standard molar volumes of H<sub>3</sub>BO<sub>3</sub>(aq) were measured at high temperatures in several laboratories,<sup>29–31</sup> indicating the predominant attractive interaction between this strongly polar solute and the aqueous media, previously considered typical only for ionic solutions. The

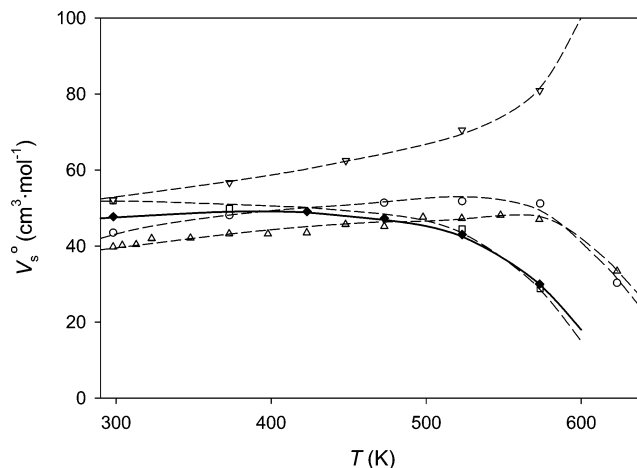


**Figure 6.** Experimental standard molar volumes  $V_s^o$  of inorganic acids at pressures close to 30 MPa. Filled diamonds, H<sub>3</sub>PO<sub>4</sub>(aq) (this study); empty squares, H<sub>3</sub>AsO<sub>4</sub>(aq) (Perfetti<sup>34</sup>); empty circles, H<sub>3</sub>AsO<sub>3</sub>(aq) (Perfetti<sup>34</sup>); empty triangles, H<sub>3</sub>BO<sub>3</sub>(aq) (Hnedkovsky et al.<sup>29</sup>); filled triangles, H<sub>3</sub>BO<sub>3</sub>(aq) (Abdulagatov and Azizov<sup>31</sup>); reversed triangles, CH<sub>3</sub>COOH(aq) (Majer et al.<sup>10</sup>). The lines are to lead the eye.

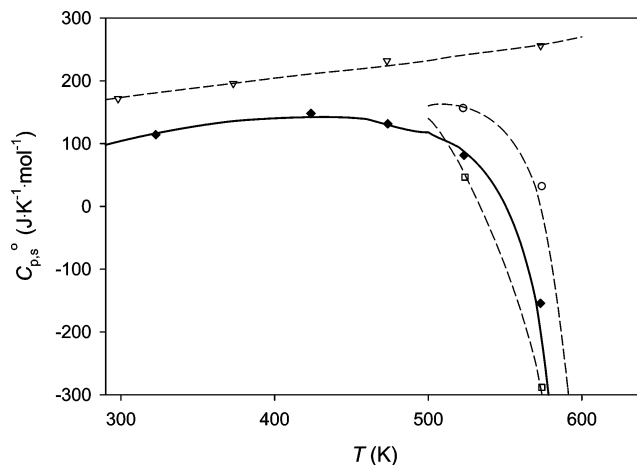


**Figure 7.** Experimental standard molar heat capacities  $C_{p,s}^o$  of inorganic acids at pressures below 20 MPa. Filled diamonds, H<sub>3</sub>PO<sub>4</sub>(aq) (this study); empty squares, H<sub>3</sub>AsO<sub>4</sub>(aq) (Perfetti<sup>34</sup>); circles, H<sub>3</sub>AsO<sub>3</sub>(aq) (Perfetti<sup>34</sup>); reversed triangles, CH<sub>3</sub>COOH(aq) (correlated data from Majer et al.<sup>10</sup>). The lines are to lead the eye.

consistent behavior was observed for the standard heat capacity of boric acid that decreases with temperatures above 500 K. Other cases were also reported later<sup>22</sup> for organic molecules with several polar substituents.<sup>32,33</sup> Data presented in this study for H<sub>3</sub>PO<sub>4</sub>(aq) confirm similar observations for this solute, as found earlier for the standard molar heat capacity by Sharygin et al.<sup>22</sup> New experimental results, analogous to the H<sub>3</sub>PO<sub>4</sub>(aq) determinations, have been recently obtained in the Clermont–Ferrand laboratory for As<sup>III</sup> and As<sup>V</sup> acids (H<sub>3</sub>AsO<sub>3</sub>(aq) and H<sub>3</sub>AsO<sub>4</sub>(aq)) and have been corrected for ionization and chemical relaxation by a similar procedure as that adopted in this study. These data now allow for a more quantitative insight into the effects of molecular size and polarity on solute behavior in aqueous solutions at superambient conditions.

Generally, the standard thermodynamic properties for all molecular forms of the studied inorganic acids display similar trends, with electrolyte-like evolution of  $V_s^o$  and  $C_{p,s}^o$  at elevated conditions (Figures 5–8). It is known that standard molar volumes at ambient conditions are typically close to molar volumes of the corresponding pure solutes. This seems to be confirmed by our data, where the standard molar volumes and heat capacities at 298 K follow approximately the order of the

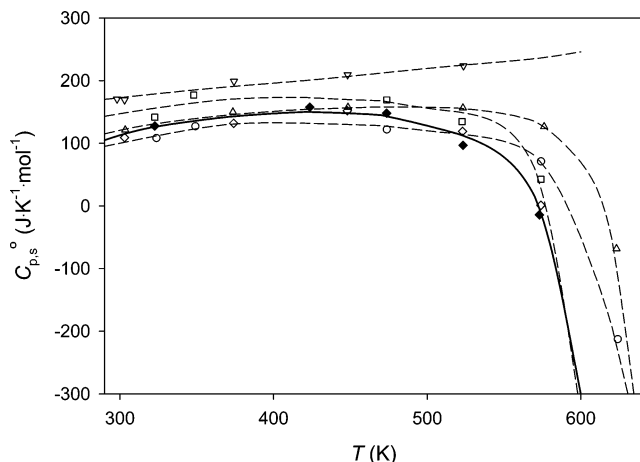


**Figure 8.** Experimental standard molar heat capacities  $C_{p,s}^{\circ}$  of inorganic acids at pressures close to 30 MPa. Filled diamonds,  $\text{H}_3\text{PO}_4(\text{aq})$  (this study); empty diamonds,  $\text{H}_3\text{PO}_4(\text{aq})$  (Sharygin et al.<sup>22</sup>); empty squares,  $\text{H}_3\text{AsO}_4(\text{aq})$  (Perfetti<sup>34</sup>); empty circles,  $\text{H}_3\text{AsO}_5(\text{aq})$  (Perfetti<sup>34</sup>); empty triangles,  $\text{H}_3\text{BO}_3(\text{aq})$  (Hnedkovsky et al.<sup>29</sup>); reversed triangles,  $\text{CH}_3\text{COOH}(\text{aq})$  (Inglese et al.<sup>35</sup>). The lines are to lead the eye.

growing molecular size:  $\text{H}_3\text{BO}_3$ ,  $\text{H}_3\text{AsO}_3$ ,  $\text{H}_3\text{PO}_4$ ,  $\text{H}_3\text{AsO}_4$ . On the other hand, the drop of the standard derivative properties of a solute is expected to be faster at high temperatures for bigger and more polar molecules. Again, this trend is confirmed by our data, with the lowest values of the standard derivative properties found for  $\text{H}_3\text{PO}_4(\text{aq})$  and the highest for  $\text{H}_3\text{BO}_3(\text{aq})$ . These regularities are undoubtedly related to the similar character of the  $\text{B}^{\text{III}}$ ,  $\text{As}^{\text{III}}$ ,  $\text{As}^{\text{V}}$ , and  $\text{P}^{\text{V}}$  acids and are not necessarily transferable to other weak acids in aqueous solution. This is documented in Figures 5–8 by the opposite behavior of  $V_s^{\circ}$  and  $C_{p,s}^{\circ}$  for acetic acid at high temperatures.<sup>10,35</sup> The volatility of this weak acid (molecular at elevated temperatures) is an indication of the positive divergence of its standard derivative properties at the critical point of water.

Basic rules governing the near-critical behavior of aqueous electrolytes and nonelectrolytes were described in the literature.<sup>36</sup> The precise volumetric and calorimetric data for dilute aqueous solutions allow one to sensitively detect the type and strength of interactions between the solute and the solvent at conditions where water is highly compressible and expansible. These findings are extremely useful, particularly when developing correlation and prediction models for the standard thermodynamic properties of weak electrolytes and highly polar nonelectrolytes where the character of the near-critical behavior is difficult to determine a priori.

**Acknowledgment.** The assistance of T. Matrab during measurements of the volumetric properties is acknowledged. J.S. was supported by the Research Centre “Advanced Remedial Technologies and Processes”; the mobility costs of V.M. and J.S. were covered by the “Barrande” bilateral project between France and the Czech Republic.

**Supporting Information Available:** Full table with original densitometric and calorimetric data, including the experimental apparent molar volumes and the apparent molar heat capacities

of  $\text{H}_3\text{PO}_4(\text{aq})$ , the calculated degrees of ionization, the corrected values of  $V_{\phi}$  and  $C_{p,\phi}$  and their error estimates. This material is available free of charge via the Internet at <http://pubs.acs.org>.

## References and Notes

- (1) Johnson, J. W.; Oelkers, E. H.; Helgeson, H. C. *Comput. Geosci.* **1992**, *18*, 899.
- (2) Tanger, J. C.; Helgeson, H. C. *Am. J. Sci.* **1988**, *288*, 19.
- (3) Shock, E. L.; Helgeson, H. C.; Sverjensky, D. A. *Geochim. Cosmochim. Acta* **1989**, *53*, 2157.
- (4) Shock, E. L.; Sassani, D. C.; Willis, M.; Sverjensky, D. A. *Geochim. Cosmochim. Acta* **1997**, *61*, 907.
- (5) Majer, V.; Sedlbauer, J.; Wood, R. H. In *Aqueous Systems at Elevated Temperatures and Pressures; Physical Chemistry in Water, Steam and Hydrothermal Solutions*; Palmer, D. A., Harvey, A. H., Fernandez-Prini, R., Eds.; Elsevier: Amsterdam, The Netherlands, 2004; pp 99–148.
- (6) Sedlbauer, J.; O’Connell, J. P.; Wood, R. H. *Chem. Geol.* **2000**, *163*, 43.
- (7) Sedlbauer, J.; Wood, R. H. *J. Phys. Chem. B* **2004**, *108*, 11838.
- (8) O’Connell, J. P. *Fluid Phase Equilib.* **1995**, *104*, 21.
- (9) O’Connell, J. P.; Sharygin, A. V.; Wood, R. H. *Ind. Eng. Chem. Res.* **1996**, *35*, 2808.
- (10) Majer, V.; Sedlbauer, J.; Hnedkovsky, L.; Wood, R. H. *Phys. Chem. Chem. Phys.* **2000**, *2*, 2907.
- (11) Archer, D. *J. Phys. Chem. Ref. Data* **1992**, *21*, 793.
- (12) Hynek, V.; Obsil, M.; Majer, V.; Quint, J. R.; Grolier, J.-P. E. *Int. J. Thermophys.* **1997**, *18*, 719.
- (13) Picker, P.; Tremblay, E.; Jolicoeur, C. *J. Sol. Chem.* **1974**, *3*, 377.
- (14) Hill, P. G. *J. Phys. Chem. Ref. Data* **1990**, *19*, 1233.
- (15) Hnedkovsky, L.; Hynek, V.; Majer, V.; Wood, R. H. *J. Chem. Thermodyn.* **2002**, *34*, 755.
- (16) Slavik, M.; Sedlbauer, J.; Ballerat-Busserolles, K.; Majer, V. *J. Solution Chem.*, in press.
- (17) Pitzer, K. S. In *Activity Coefficients in Electrolyte Solutions*; Pitzer, K. S., Ed.; CRC Press: Boca Raton, FL, 1991.
- (18) Archer, D. G.; Wang, P. J. *J. Phys. Chem. Ref. Data* **1990**, *19*, 371.
- (19) Holmes, H. F.; Mesmer, R. E. *J. Solution Chem.* **1999**, *28*, 327.
- (20) Jolicoeur, C.; Hemelin, L. L.; Lapalme, R. *J. Phys. Chem.* **1979**, *83*, 2806.
- (21) Larson, J. W.; Zeeb, K. G.; Hepler, L. G. *Can. J. Chem.* **1982**, *60*, 2141.
- (22) Sharygin, A. V.; Inglese, A.; Sedlbauer, J.; Wood, R. H. *J. Solution Chem.* **1997**, *26*, 183.
- (23) Mesmer, R. E.; Baes, C. F. *J. Solution Chem.* **1974**, *3*, 307.
- (24) Read, A. J. *J. Solution Chem.* **1988**, *17*, 213.
- (25) Sedlbauer, J.; Majer, V. *Eur. J. Mineral.* **2000**, *12*, 1109.
- (26) Sedlbauer, J.; Bergin, G.; Majer, V. *AIChE J.* **2002**, *48*, 2396.
- (27) Wagman, D. D.; Evans, W. H.; Parker, V. B.; Schumm, R. H.; Halow, I.; Bailey, S. M.; Churney, K. L.; Nuttall, R. L. *J. Phys. Chem. Ref. Data* **1982**, *11*, 1.
- (28) Chase, M. W. (Editor) *J. Phys. Chem. Ref. Data* **1998**, *27*, I–II.
- (29) Hnedkovsky, L.; Majer, V.; Wood, R. H. *J. Chem. Thermodyn.* **1995**, *27*, 801.
- (30) Ganopolsky, J. G.; Bianchi, H. L.; Corti, H. R. *J. Solution Chem.* **1996**, *25*, 391.
- (31) Abdulgatov, I. M.; Azizov, N. D. *J. Solution Chem.* **2004**, *33*, 1305.
- (32) Bulemela, E.; Tremaine, P. R. *J. Phys. Chem. B* **2005**, *109*, 20539.
- (33) Censky, M.; Hnedkovsky, L.; Majer, V. *J. Chem. Thermodyn.* **2005**, *37*, 221.
- (34) Perfetti, E. M.S. Thesis, Blaise Pascal University, Clermont-Ferrand, 2003.
- (35) Inglese, A.; Sedlbauer, J.; Wood, R. H. *J. Solution Chem.* **1996**, *25*, 849.
- (36) Anisimov, M. A.; Sengers, J. V.; Levelt Sengers, J. M. H. In *Aqueous Systems at Elevated Temperatures and Pressures; Physical Chemistry in Water, Steam and Hydrothermal Solutions*; Palmer, D. A., Harvey, A. H., Fernandez-Prini, R., Eds.; Elsevier: Amsterdam, The Netherlands, 2004; pp 29–72.